PRL **105,** 266102 (2010) PHYSICAL REVIEW LETTERS week ending 31 DECEMBER 2010

Reversible Bond Formation in a Gold-Atom–Organic-Molecule Complex as a Molecular Switch

Fabian Mohn,[1,*] Jascha Repp,[2,1] Leo Gross,[1] Gerhard Meyer,[1] Matthew S. Dyer,[3] and Mats Persson[3,4]
[1]*IBM Research–Zurich, 8803 Rüschlikon, Switzerland*
[2]*Institute of Experimental and Applied Physics, University of Regensburg, 93040 Regensburg, Germany*
[3]*Surface Science Research Centre, Department of Chemistry, University of Liverpool, Liverpool, L69 3BX, United Kingdom*
[4]*Department of Applied Physics, Chalmers University of Technology, SE-412 96, Göteborg, Sweden*

(Received 16 September 2010; published 28 December 2010)

We report on the formation of a metal-molecule complex that can be used as a molecular switch. Using a cryogenic scanning tunneling microscope, a covalent bond was formed reversibly between a gold atom and a perylene-3,4,9,10-tetracarboxylic dianhydride molecule supported by a thin insulating film. The bonded and the nonbonded state of the complex were found to be associated with different charge states, and the switching between the two states was accompanied by a considerable change in the tunneling current. Atomic force microscopy molecular imaging was employed to determine precisely the atomic structure of the complex, and the experimental results were corroborated by density functional theory calculations.

DOI: 10.1103/PhysRevLett.105.266102 PACS numbers: 68.37.Ef, 68.37.Ps, 71.15.Mb, 82.37.Gk

The concept of using single atoms and molecules as memory elements or switches in electronic devices was established long ago [1]. Scanning tunneling microscopy (STM) has been used to investigate and identify promising molecular switches [2–7], due to its capabilities to image and manipulate adsorbates on the atomic scale. Atomic manipulation was also performed with noncontact atomic force microscopy (AFM) a few years ago [8–10], and most recently it was shown that atomic resolution can be achieved on organic molecules by functionalizing an AFM tip with a suitable atomic termination [11]. STM has repeatedly been used for the making and breaking of single chemical bonds between metal atoms and molecules [12–16] and between molecules [17,18]. Those previous examples of bond formation, however, were not suited as molecular switches, because they required complex protocols of STM tip positioning, voltage pulses or current injection, involved various possible configurations of the constituents, or resulted in only a slight change of the tunneling current. Furthermore, in the examples mentioned it was not possible to switch between the bonded and the nonbonded state in a reliable and directed manner (meaning that the system can be switched with certainty to the desired state).

In this Letter, we present a molecular switch that is based on the reversible bond formation between a Au adatom and an organic admolecule [perylene-3,4,9,10-tetracarboxylic dianhydride (PTCDA)] on a thin NaCl film supported by a Cu substrate. The switching between the bonded and the nonbonded configuration was accompanied by a change in the tunneling current of about 2 orders of magnitude. The bond making and breaking were controlled simply by applying voltage pulses of according polarity and did not require an exact tip movement or positioning over a particular part of the molecule. The operation and electronic characterization of the switch were performed with STM, whereas the exact geometry of the complex was deduced from atomically resolved AFM images. The experimental results were combined with density functional theory (DFT) calculations to gain further insight into the details of the bonding geometry and the electronic structure of the complex. Our results strongly suggest that the reliability and directed manner of the switching are based on the fact that a change of the charge state of the complex occurs upon bond formation. The electronic decoupling provided by the insulating NaCl film is crucial to ensure the stability of the different charge states [5,19].

Our experiments were performed with a homebuilt combined STM/AFM system using a qPlus tuning fork sensor [20] operated in UHV and at low temperature ($T_{\text{sample}} \approx 5$ K). NaCl was evaporated onto a clean Cu(111) single-crystal surface at $T_{\text{sample}} \approx 270$ K, leading to the formation of (100)-terminated islands of mostly two atomic layers in thickness, denoted as NaCl(2ML)/Cu(111) [21]. Low coverages of Au atoms and PTCDA molecules were then evaporated *in situ* at $T_{\text{sample}} \approx 10$ K. The tip preparation techniques described in Ref. [11] were employed to obtain well-defined tips for our STM and AFM investigations.

In Fig. 1, the reversible switching of a Au-PTCDA complex on NaCl(2ML)/Cu(111) is shown. First of all, we used vibrational excitation by inelastic electron tunneling into a negatively charged Au adatom (identified in the STM image by its characteristic surrounding depression [19]) to successively move it towards a PTCDA molecule. Once the Au^- and the PTCDA had been positioned close enough to each other [Fig. 1(a)], it was possible to switch the complex to a different state by ramping the sample bias voltage to $V = -1.5$ V [Fig. 1(b)]. The switching process was found to be completely reversible [Fig. 1(c)]. In the

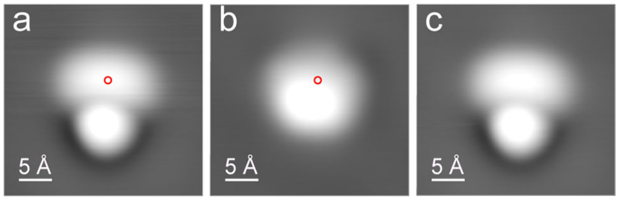

FIG. 1 (color online). Reversible switching of a Au-PTCDA complex. (a) Au^- adatom in close proximity of a PTCDA admolecule. With the tip at the position indicated by the (red) circle, the bias voltage V was ramped to -1.5 V. A sudden increase in the tunneling current I indicated a successful modification of the complex. (b) In the subsequent STM image, the adatom and the molecule no longer appear separated. By ramping the voltage to $+1.5$ V, the complex was switched back to the initial state, as confirmed by the subsequent image (c). Imaging parameters: $I = 5$ pA, $V = 0.2$ V.

following, we will refer to the two different states of the complex in Fig. 1(a) and 1(b) as the nonbonded [Au-PTCDA(N)] and the bonded [Au-PTCDA(B)] configuration, respectively.

We studied the adsorption sites, charge states, and the electron and hole addition spectra of single PTCDA molecules and the two configurations of Au-PTCDA using STM imaging and spectroscopy. The adsorption sites were determined from STM images with atomically resolved substrate. We found that PTCDA adsorbs in two different geometries, with the long molecule axis oriented either along the polar ⟨011⟩ or the nonpolar ⟨001⟩ atomic rows of the NaCl(100) surface. In both cases the molecule is centered on a Cl site, in agreement with previous studies [22,23]. The ⟨011⟩ orientation was found to prevail, and all experimental and theoretical data presented in this Letter were obtained for this adsorption geometry.

The charge state of adsorbates on NaCl(2ML)/Cu(111) is revealed by the scattering wave pattern of the substrate's interface state [19]. A single PTCDA molecule was found to scatter the interface electrons to a similar extent as a Au^- adatom. Considering that the affinity energy of PTCDA ($E_A \approx 4.6$ eV [24]) is substantially greater than the work function of the substrate ($\Phi \approx 3.9$ eV [25]), we propose that PTCDA becomes singly negatively charged upon adsorption. For Au-PTCDA(N), the sombrero-shaped appearance of the Au atom indicates that it is negatively charged. The observed scattering pattern around Au-PTCDA(N), however, cannot be reconciled with the assumption that only the Au atom is charged, indicating that the entire complex is doubly negatively charged. When we switched the complex, we observed a clear change in the scattering wave pattern, with Au-PTCDA(B) still exhibiting the characteristic scattering of a charged species. A comparison with scattering patterns of single Au^- adatoms suggests that Au-PTCDA(B) is singly negatively charged [26].

The electronic structure of the different states of the complex was further investigated by dI/dV spectroscopy and STM imaging [27]. The dI/dV spectrum of a single PTCDA molecule on NaCl(2ML)/Cu(111) has a distinct peak at $V \approx 0.8$ V, which we attribute to electron tunneling from the tip into the singly occupied molecular orbital (SOMO) of $PTCDA^-$ [28]. The two configurations of Au-PTCDA exhibited distinctively different spectra, as can be seen from the I-V curve shown in Fig. 2. For Au-PTCDA (N), a high current was measured only for voltages above $+0.6$ V, whereas for Au-PTCDA(B), a high current was measured below -0.6 V. The corresponding orbital images are shown in the insets of Fig. 2, together with an image of the SOMO of a single $PTCDA^-$ admolecule [30]. For Au-PTCDA(N), the image is simply given by the superposition of the image of the SOMO of $PTCDA^-$ and a circular protrusion at the position of the Au^- adatom. For Au-PTCDA(B), on the other hand, the orbital was found to be strongly distorted with an additional diagonally oriented nodal plane, in agreement with DFT calculations [26]. This indicates a strong coupling between the electronic states of the molecule and the Au atom, which is characteristic of the formation of a covalent bond. Furthermore, it was found that there exist two equivalent mirrored configurations of Au-PTCDA(B) (lower insets in Fig. 2). Note that the I-V curve in Fig. 2 represents a complete switching cycle, demonstrating directed switching from the bonded to the nonbonded configuration and back. The switching was found to be highly reproducible; i.e., the complex could be switched back and forth several dozens of times, with only minor variations (< 0.1 V) in the switching voltage.

To determine the atomic structure of the different configurations of Au-PTCDA, we used atomically resolved

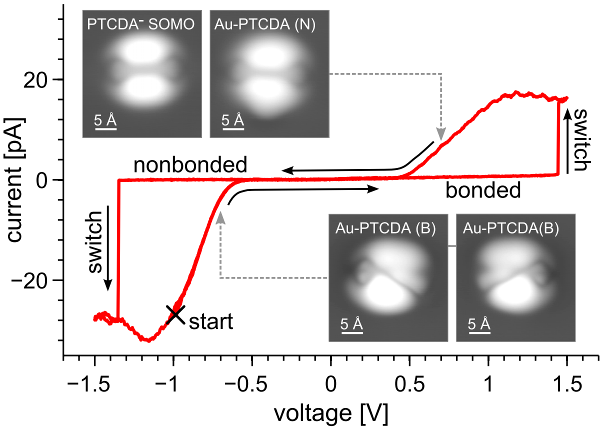

FIG. 2 (color online). Switching cycle of Au-PTCDA. The I-V curve was measured above the center of the complex and the voltage cycling is indicated by the arrows. Initially, the complex was in the bonded configuration. No peak was seen at positive bias before the switching to the nonbonded configuration occurred at $V \approx 1.4$ V. For Au-PTCDA(N), on the other hand, the current at negative bias was suppressed. The insets show STM orbital images of PTCDA and the different states of Au-PTCDA, recorded at $I = 5$ pA and $V = +0.8$ V for PTCDA, $V = +0.7$ V for Au-PTCDA(N), and $V = -0.7$ V for Au-PTCDA(B).

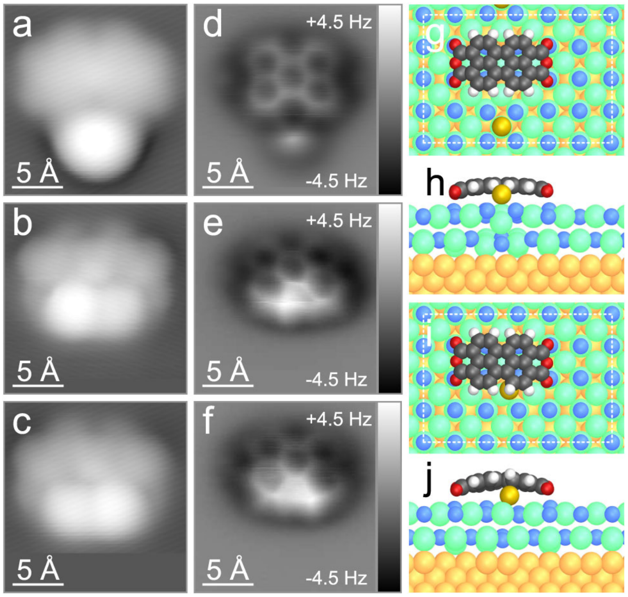

FIG. 3 (color online). Bonding geometry of Au-PTCDA. (a)–(c) STM images of Au-PTCDA in the nonbonded [(a)] and the bonded [(b),(c)] configuration (imaging parameters: $I = 3$ pA, $V = 0.2$ V). The tip had been terminated with a CO molecule. (d)–(f) Corresponding constant-height AFM images (imaging parameters: amplitude $A = 0.4$ Å, frequency $f = 23, 165$ Hz and distance with respect to the STM set point above the substrate between $+0.8$ Å and $+1.0$ Å). (g)–(j) DFT-calculated geometries of the complex in the nonbonded [(g),(h)] and the bonded [(i),(j)] state. The unit cell used for the calculations is indicated in (g) and (i), and the different atomic species are colored in gray (C), red (O), white (H), green (Cl), blue (Na), orange (Cu), and yellow (Au) in the online color version.

AFM molecular imaging [11]. The images were acquired at constant height with a CO-terminated tip, which yielded enhanced resolution also in topographical STM imaging [Figs. 3(a)–3(c)]. In the corresponding AFM images [Figs. 3(d)–3(f)], the perylene core of the PTCDA is clearly resolved, in contrast to the STM images. For Au-PTCDA(N), the AFM image shows that the molecule and the adatom are clearly separated, with the distance between the Au atom and the center of the central carbon ring of the PTCDA being close to twice the Cl-Cl distance in the topmost NaCl layer. After switching to Au-PTCDA(B), in both the STM and the AFM images we observe that, while the PTCDA basically maintains its position, the Au atom no longer appears separated from the molecule. In the AFM images of Au-PTCDA(B), the brightness of the lower part of the atom-molecule complex is enhanced, which corresponds to a stronger Pauli repulsive force and indicates that this region of the molecule is closer to the tip [11]. A distinct maximum of the repulsive interaction is observed above one of the two inner C sites at the lower edge of the molecule, and the two mirrored configurations can be clearly distinguished.

To gain more detailed insight into the nature of the switchable atom-molecule complex, we have carried out periodic DFT calculations, using the projector augmented wave method [31] as implemented in the plane-wave-based VASP code [32]. Exchange-correlation effects were described by the generalized gradient approximation [33]. As the (100)-terminated NaCl bilayer is incommensurate with the Cu(111) surface, we carried out calculations for the closely related system NaCl(2ML)/Cu(100), for which the NaCl bilayer lattice is in good match with the Cu(100) surface lattice [34]. The metal support was modeled by a four-layer slab of Cu atoms, the vacuum region was about 17.5 Å in height, and the surface unit cell is shown in Fig. 3. The full structural optimization of all the ion cores except the two bottom layers of the Cu slab was carried out using a plane wave cutoff of 400 eV on a $2 \times 2 \times 1$ k-point grid, until the forces acting on the ion cores were smaller than 0.03 eV/Å.

The calculated atomic structures of the complex in the different configurations [Figs. 3(g)–3(j)] corroborate the conclusions drawn from the atomically resolved AFM images. The PTCDA was found to be centered on a Cl ion, with the oxygen end groups bent towards the substrate (this might explain why these atoms are not visible in the AFM images), similar to the situation on metal surfaces [35]. A stable configuration was found with the Au atom adsorbed on top of a Cl^- ion two atom rows away from the adsorbed PTCDA molecule, which corresponds to the observed nonbonded configuration. Bringing the Au atom closer to the molecule, we found two equivalent configurations with the atom bonded to the adsorbed PTCDA molecule. The Au atom is one Cl site closer to the molecule than in Au-PTCDA(N) and bonds to a Cl^- ion and a C atom by tilting the H atom away from the molecular plane, indicating an sp^2 to sp^3 rehybridization [13]. This tilting is consistent with the enhanced brightness observed above one of the C sites at the lower edge of the molecule in Figs. 3(e) and 3(f).

A more detailed account of the charge states and the bonding is given by the calculated partial densities of states (DOS) of the s and p_z partial waves around the Au atom and all the C atoms of the Au-PTCDA complex, respectively, see Fig. 4. For Au-PTCDA(N), the partial DOS of the s and p_z partial waves are essentially the same as for the single Au adatom and the single PTCDA admolecule. This shows that no covalent bond is formed between the two species. Upon adsorption, the lowest unoccupied molecular orbital of the PTCDA molecule, being of π character, becomes a SOMO partially occupied by one electron and the 6s state of the Au atom becomes fully occupied. This result confirms the assumption that Au-PTCDA(N) is doubly charged. In contrast, the partial DOS for Au-PTCDA(B) indicates the formation of a covalent bond arising from the strong mixing of the Au 6s state with the π orbitals of the PTCDA admolecule. In this case, there are no partially occupied orbitals and the calculations show that Au-PTCDA(B) is occupied with one electron less than Au-PTCDA(N), which confirms that Au-PTCDA(B) is singly charged.

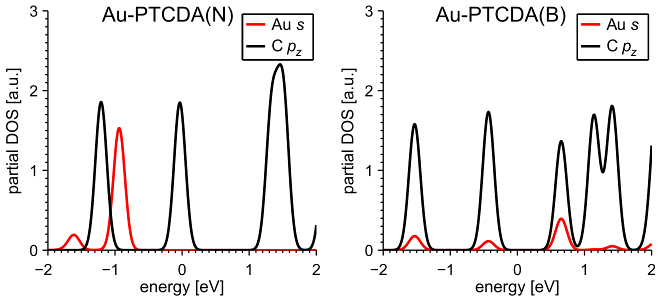

FIG. 4 (color online). Calculated partial densities of electronic states of s and p_z partial waves around the Au atom and all the C atoms in the two configurations of the Au-PTCDA complex on NaCl(2ML)/Cu(100). The energies are given with respect to the Fermi level $E_F = 0$ eV.

The picture emerging from our combined experimental and theoretical study suggests a simple mechanism for the switching of the Au-PTCDA complex: the attachment of a long-lived hole at negative bias to the SOMO state of the PTCDA$^-$ in the Au-PTCDA(N) complex reduces the Coulomb repulsion between the Au$^-$ and the PTCDA$^-$, which enables the adatom to change its position and form a bond with the molecule [36]. Reversibly, the attachment of a long-lived electron to the LUMO state of the singly negatively charged Au-PTCDA(B) causes a Coulomb repulsion between the adatom and the molecule, which results in a breaking of the bond. This mechanism seems to be much more reliable than bond activation by inelastic electron tunneling.

In conclusion, we have demonstrated that the reversible bond formation between a Au adatom and a PTCDA admolecule on NaCl(2ML)/Cu(111) acts as a molecular switch with a tunneling current on/off ratio of about 2 orders of magnitude. The high reliability of the switching is attributed to long-lived electron or hole attachments to the Au-PTCDA complex, which make it possible to cross the barrier between the bonded and the nonbonded configuration on an excited state potential energy surface.

Valuable comments from R. Allenspach, financial support from the EU projects HERODOT and ARTIST, the Volkswagen Foundation through its Lichtenberg program, the Swedish Research Council (VR), and computing resources provided by SNIC and University of Liverpool are gratefully acknowledged.

---

*fmo@zurich.ibm.com

[1] A. Aviram and M. A. Ratner, Chem. Phys. Lett. **29**, 277 (1974).
[2] J. Henzl *et al.*, Angew. Chem., Int. Ed. **45**, 603 (2006).
[3] B.-Y. Choi *et al.*, Phys. Rev. Lett. **96**, 156106 (2006).
[4] M. J. Comstock *et al.*, Phys. Rev. Lett. **99**, 038301 (2007).
[5] S. W. Wu, N. Ogawa, and W. Ho, Science **312**, 1362 (2006).
[6] P. Liljeroth, J. Repp, and G. Meyer, Science **317**, 1203 (2007).
[7] Y. Wang *et al.*, J. Am. Chem. Soc. **131**, 3639 (2009).
[8] Y. Sugimoto *et al.*, Nature Mater. **4**, 156 (2005).
[9] Y. Sugimoto *et al.*, Science **322**, 413 (2008).
[10] M. Ternes *et al.*, Science **319**, 1066 (2008).
[11] L. Gross *et al.*, Science **325**, 1110 (2009).
[12] H. J. Lee and W. Ho, Science **286**, 1719 (1999).
[13] J. Repp *et al.*, Science **312**, 1196 (2006).
[14] D. Wegner *et al.*, Phys. Rev. Lett. **103**, 087205 (2009).
[15] P. Liljeroth *et al.*, Nano Lett. **10**, 2475 (2010).
[16] R. Ohmann, L. Vitali, and K. Kern, Nano Lett. **10**, 2995 (2010).
[17] S.-W. Hla *et al.*, Phys. Rev. Lett. **85**, 2777 (2000).
[18] T. Kumagai *et al.*, Phys. Rev. Lett. **100**, 166101 (2008).
[19] J. Repp *et al.*, Science **305**, 493 (2004).
[20] F. J. Giessibl, Appl. Phys. Lett. **76**, 1470 (2000).
[21] R. Bennewitz *et al.*, Surf. Sci. **438**, 289 (1999).
[22] O. H. Pakarinen *et al.*, Phys. Rev. B **80**, 085401 (2009).
[23] E. Le Moal *et al.*, Phys. Rev. B **82**, 045301 (2010).
[24] T. Chassé *et al.*, J. Appl. Phys. **85**, 6589 (1999).
[25] R. Bennewitz *et al.*, Surf. Interface Anal. **27**, 462 (1999).
[26] See supplementary material at http://link.aps.org/supplemental/10.1103/PhysRevLett.105.266102 for STM images of the interface state scattering and calculated orbital images of Au-PTCDA.
[27] J. Repp *et al.*, Phys. Rev. Lett. **94**, 026803 (2005).
[28] At voltages around −1 V, we also observed a peak, which we ascribe to bipolar tunneling [29], because this peak shifted when varying the tip-sample distance and the corresponding orbital images were similar to the SOMO image at positive bias, but strongly tip dependent.
[29] S. W. Wu *et al.*, Phys. Rev. Lett. **93**, 236802 (2004).
[30] For simplicity, we refer to STM images recorded at voltages corresponding to peaks in the dI/dV spectrum of a molecule as orbital images, because of their close resemblance to contours of constant orbital density [27].
[31] G. Kresse and D. Joubert, Phys. Rev. B **59**, 1758 (1999).
[32] G. Kresse and J. Furthmüller, Phys. Rev. B **54**, 11 169 (1996).
[33] J. P. Perdew *et al.*, Phys. Rev. B **46**, 6671 (1992).
[34] We are well aware of the fact that the different work function of NaCl(2ML)/Cu(100) could have an influence on the stability of different charge states. A more detailed discussion of this problem is given in Ref. [26].
[35] A. Hauschild *et al.*, Phys. Rev. Lett. **94**, 036106 (2005).
[36] Bond activation by inelastic excitation of the adatom as in Ref. [13] is unlikely, since the Au atom reliably moved to the PTCDA molecule also when tunneling out of the molecular resonance far away from the adatom, at the opposite end of the molecule.